1 Preliminary studies

1.1 Homogeneous vs heterogeneous isotope distribution

This study modeled two different isotope distributions in a fuel compact. First, a homogeneous distribution of the isotopes. Second, a heterogeneous distribution, in which we explicitly model the TRISO particles. We modeled both cases using Serpent. We used a hexagonal unit cell model that includes the fuel compact, a helium gap, and the surrounding graphite. Table **??** specifies the model input parameters. The material temperature was 1200K, case that represents the Hot Full Power (HFP) core state. Serpent ran 5×10^4 neutrons/cycle, 500 active cycles, and 50 inactive cycles for the calculations. The simulations took 1.73 and 2.21 minutes using 256 cores. The heterogeneous calculations took a 28% more.

The multiplication factor was 1.17523 for the homogeneous case and 1.25106 for the heterogeneous case. Using the heterogeneous case as the reference result, we calculated the relative error of the most relevant group constants in an eigenvalue calculation. Serpent generated the group constants using the three energy group structure in Table 1. The evaluated parameters were D_g, Σ_g^r, $\nu\Sigma_g^f$, and χ_g^t (see equation **??**). Figure 1 displays the relative errors for Σ_g^r and $\nu\Sigma_g^f$, which were the group constants that changed the most. The figure does not include relative errors for D_g and χ_g^t because they were less than 1%. The relative errors of Σ_g^r and $\nu\Sigma_g^f$ were less than 6%.

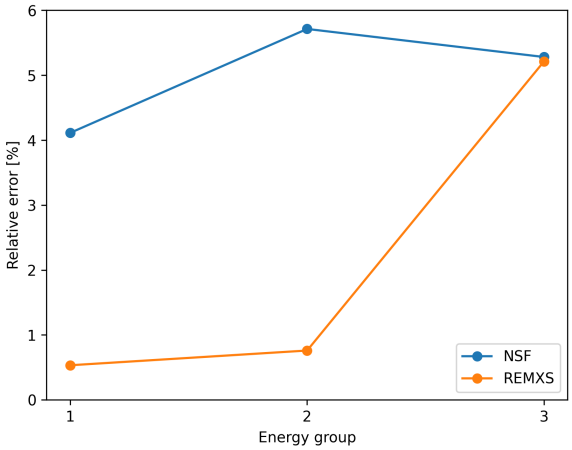

Figure 1: Relative error of the group constants generated with a homogeneous isotope distribution.

1.2 Moltres limitations

Serpent run 5×10^5 neutrons/cycle, 400 active cycles, and 100 inactive cycles for the calculations. The multiplication factor was 1.41933.

Moltres Mesh: dof/group () Keff =

Figures

2 Conclusions

The preliminary studies focused on several aspects of the simulations. The first aspect was the effect of distributing homogeneously the fuel compact isotopes in the Serpent model. The heterogeneous calculation took 28% more time. The results showed that the multiplication factor decreases considerably. Additionally, the homogenization of the fuel compact appears not to have a strong impact over the group constants. However, the

considerable difference in the multiplication factor suggests that the combined effect of small variations in the group constants is significant. Although the particles' explicit modeling is time-consuming, it results necessary.

Based on these results and discussions, in the following sections, we obtain the homogenized group constants. In the fuel block, the fuel, coolant, and moderator all share the same group constants.

3 Serpent-Moltres validation

3.1 Fuel column

In this section, we investigated the effects of the choice of energy group structure on the diffusion simulations. We conducted two analyses. First, we varied the number of energy groups. Second, we tried different energy group structures for the same number of groups. To reduce the computational expense we narrowed down our focus to a fuel column of the MHTGR, Figure 2. The fuel column includes the bottom and top reflectors. Tables **??** and **??** specify the model input parameters.

The first step in the calculation was to obtain the group constants using Serpent. Figure 2 displays xy-plane of the model. High Temperature Gas-Cooled Reactors (HTGRs) use Lumped Burnable Poisons (LBPs) to reduce the peaking factors in different regions of the active core. Some reactors could have LBPs in the rings closer to the reflectors, and no LBPs in the middle rings. This motivated the analysis of two cases, a fuel column that does not have LBPs, and one that has. The material temperatures were 600K and 1200K, cases that represent the Cold Zero Power (CZP) and the HFP core states. Serpent ran 4×10^5 neutrons/cycle, 360 active cycles, and 40 inactive cycles for the calculations.

We made the geometry and mesh using Gmsh [1]. Taking advantage of the symmetry of the problem, the model included only a one-twelfth of the fuel column. The mesh had 37120 elements and 22862 nodes. The diffusion calculations had 22862 Degree of Freedoms (DoFs)/energy-group. The Moltres input files set an eigenvalue and a flux convergence tolerance of 1×10^{-8}. The calculations in Moltres used different energy group structures listed in Table 1.

To compare the results from Serpent and Moltres, we present a figure comparing the three-group axial flux. Moltres ran the calculations for 26 energy groups, and collapsed the results to three energy groups to facilitate the visualization of the results. Note that the flux in Serpent is an average over the volume, while the flux in Moltres is the point-wise flux over a line. Another figure compares the eigenvalue from Serpent and eigenvalues from Moltres for the different energy group structures. The last analysis is for the Moltres axial flux. Considering the 26 group structure as the reference value, we obtained the L2-norm relative error for the axial flux in the active core.

To recapitulate, we simulated four operational cases: no LBP and 600K, no LBP and 1200K, LBP and 600K, and LBP and 1200K. Figures 3 to 6 display the axial flux from the Serpent and the Moltres simulations for all cases. For the no LBP at 600K case, the fluxes are close in shape and magnitude. For the no LBP at 1200K case, the fluxes look similar. The flux in Moltres has a more straight shape. The thermal flux peak in the bottom reflector has a bigger magnitude. For the LBP at 600K case, the flux in Moltres has a bigger magnitude. Additionally, the shape of the Moltres flux is concave while the Serpent flux is convex. For the LBP at 1200K case, the flux in Moltres is bigger. The Moltres flux is more concave than the Serpent flux. Overall, the fluxes in Moltres and Serpent are close.

Table 2 exhibits the reactivity difference ($\Delta\rho$) between the Serpent and Moltres eigenvalues. We used equation 1 to obtain $\Delta\rho$. The eigenvalues in Moltres differ slightly from the eigenvalues in Serpent. Overall, the reactivity difference is less than 50 pcm. We note that the number of energy groups does not affect the accuracy of the eigenvalue calculations in Moltres.

$$\Delta\rho = \left| \frac{k_1 - k_2}{k_1 k_2} \right| \tag{1}$$

where

$$k_1 = \text{Serpent eigenvalue}$$
$$k_2 = \text{Moltres eigenvalue} \tag{2}$$

Figures 7 and 8 show the L_2-norm relative error for the different energy group structures. We note that the relative error for the no LBP case is smaller than the relative error of the LBP case. Overall, the relative error decreases with an increase in the number of energy groups. Nonetheless, this is not always the case. For example, in Figure 7b, going from 12 to 15 groups, the thermal flux improves, but the fast flux worsens. Additionally, we observe that a low number of energy groups yields an error of more than a 100%. In which, case we can conclude that the solution is wrong.

We added to the analysis the computational time and the peak memory usage during the simulations, Figure 9. All the simulations used 128 cores. We present only the cases at 600K because the change in temperature does not have a significant impact. The computational requirements rises with an increase in the number of energy groups. As the geometry uses a constant number of elements, the DoFs/energy-group is constant. Thus, the number of DoFs is proportional to the number of energy groups. We also discern that the overall time of the LBP cases is higher than the no LBP cases.

Finally, we analyzed the impact of changing the energy group structure for a constant number of energy groups. We chose 15 energy groups, as it gives an overall good accuracy and a not so high computational expense.

Table 1 holds the different energy group structures. Table 3 exhibits the results.

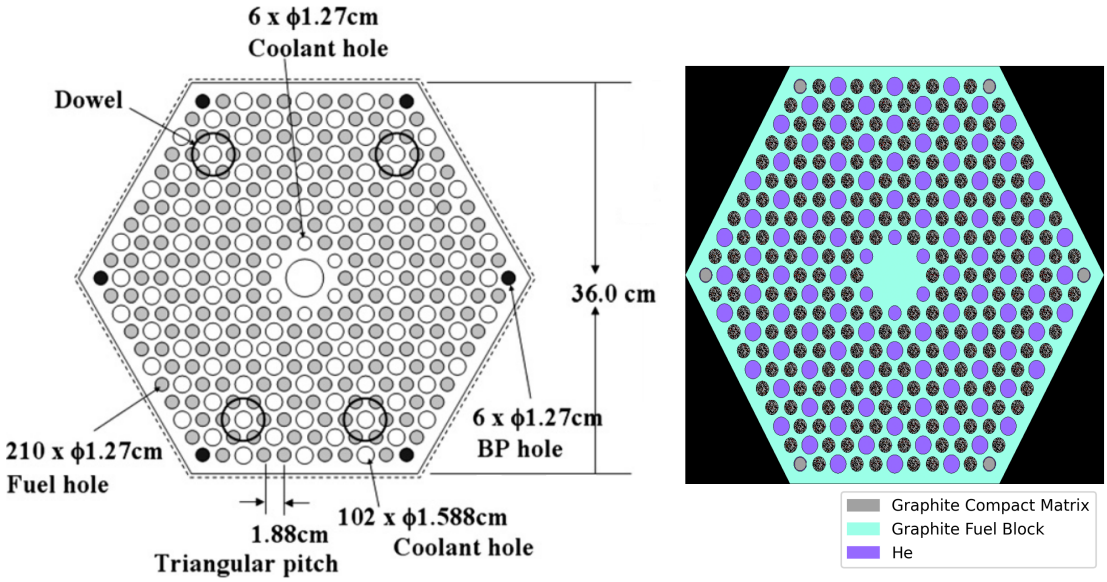

(a) Fuel column geometry. Image reproduced form [2].

(b) Serpent model geometry.

Figure 2: Fuel column of the MHTGR-350. XY-plane in the active core region.

3.2 Full-core

Table 1: Energy group structure.

Upper boundary [eV]	26	21	18	15a	15b	15c	15d	15e	12	9	6	3
1.49E+07	1	1	1	1	1	1	1	1	1	1	1	1
7.41E+06	2											
3.68E+06	3	2	2	2	2	2	2	2	2			
6.72E+05	4											
1.11E+05	5	3	3	3	3	3	3	3	3	2	2	2
1.93E+04	6	4	4	4	4				4			
3.35E+03	7											
1.58E+03	8	5	5			4						
7.48E+02	9	6	6	5	5		4	4	5	3		
2.75E+02	10	7	7	6	6	5			6	4		
1.30E+02	11	8	8	7	7		5	5	7	5	3	
6.14E+01	12	9			8	6						
2.90E+01	13	10	9	8	9		6	6				
1.37E+01	14	11	10	9					8	6		
8.32E+00	15	12	11	10	10	7	7	7	9			
5.04E+00	16											
2.38E+00	17	13	12	11	11	8	8	8	10	7	4	3
1.29E+00	18	14										
6.50E-01	19	15	13	12	12	9	9	9	11	8	5	
3.50E-01	20	16				10	10					
2.00E-01	21	17	14	13	13	11	11	10				
1.20E-01	22							11				
8.00E-02	23	18	15	14	14	12	12	12				
5.00E-02	24	19	16			13	13	13				
2.00E-02	25	20	17	15	15	14	14	14	12	9	6	
1.00E-02	26	21	18			15	15	15				

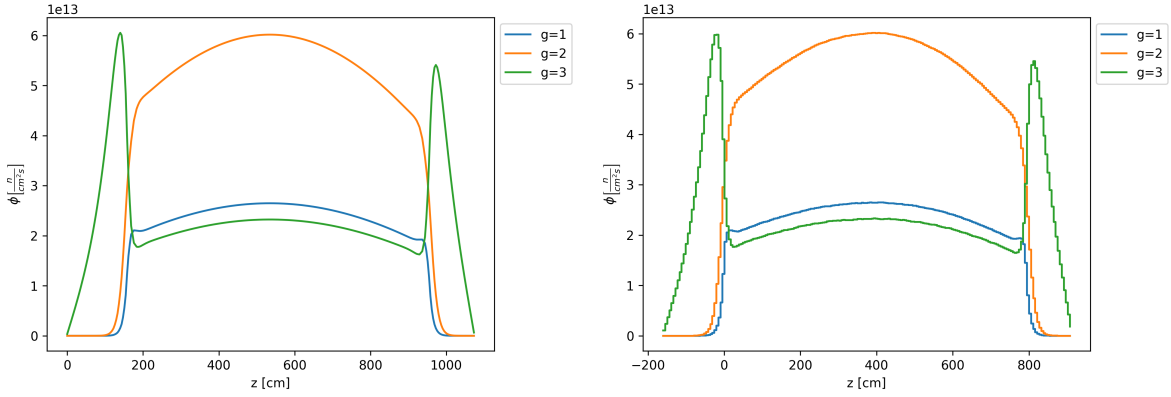

(a) Moltres.

(b) Serpent.

Figure 3: Case no LBP at 600K. 3-group axial neutron flux.

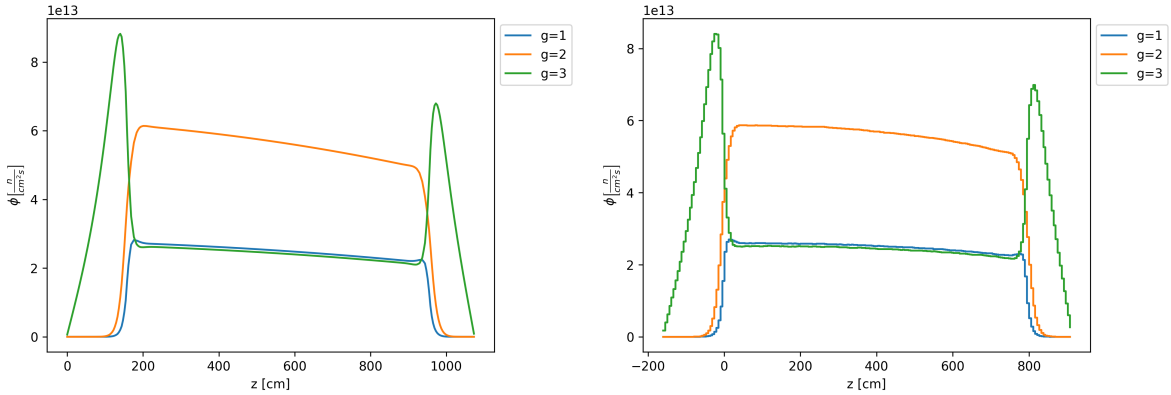

(a) Moltres. (b) Serpent.

Figure 4: Case no LBP at 1200K. 3-group axial neutron flux.

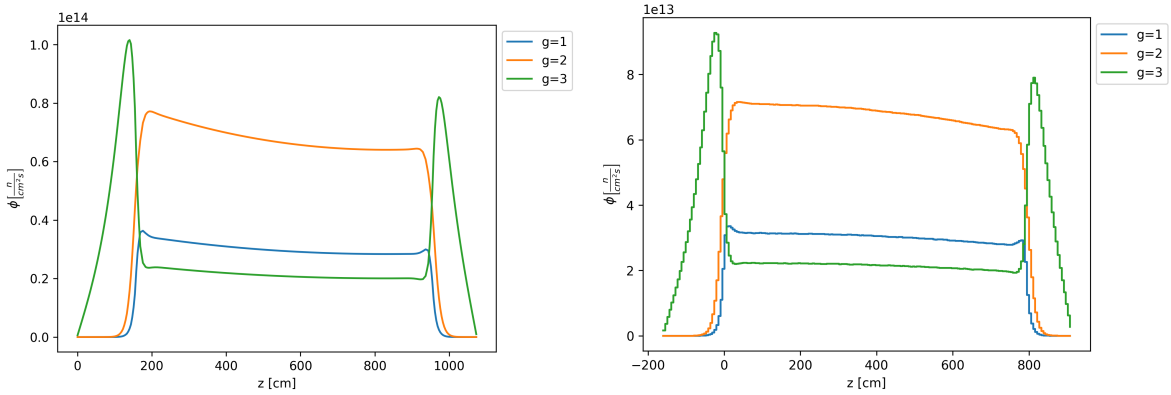

(a) Moltres. (b) Serpent.

Figure 5: Case LBP at 600K. 3-group axial neutron flux.

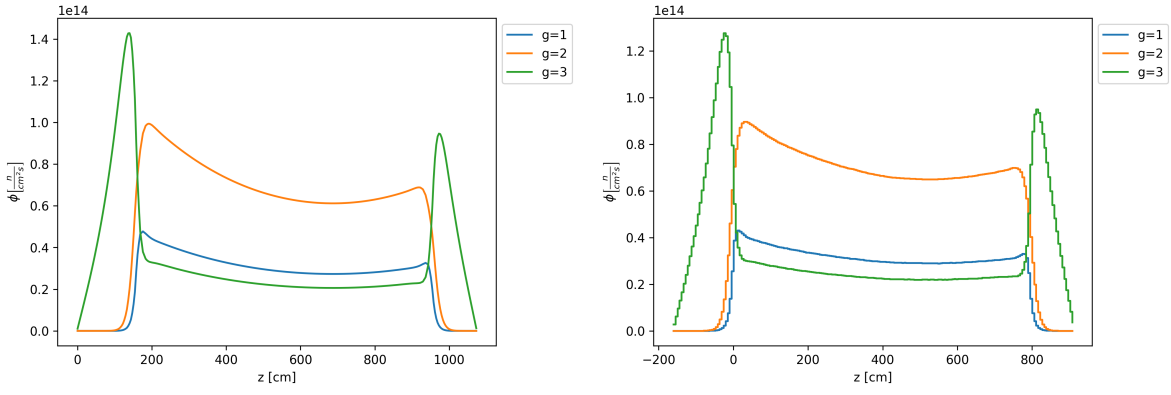

(a) Moltres. (b) Serpent.

Figure 6: Case LBP at 1200K. 3-group axial neutron flux.

Table 2: Serpent and Moltres eigenvalues.

	Serpent	$\Delta\rho$ [pcm]							
		3	6	9	12	15	18	21	26
no LBP, 600K	1.43800	10	7	6	6	5	6	6	12
no LBP, 1200K	1.37771	23	15	4	3	2	2	1	11
LBP, 600K	1.12861	44	21	24	25	25	24	19	9
LBP, 1200K	1.06554	36	40	29	32	44	43	25	25

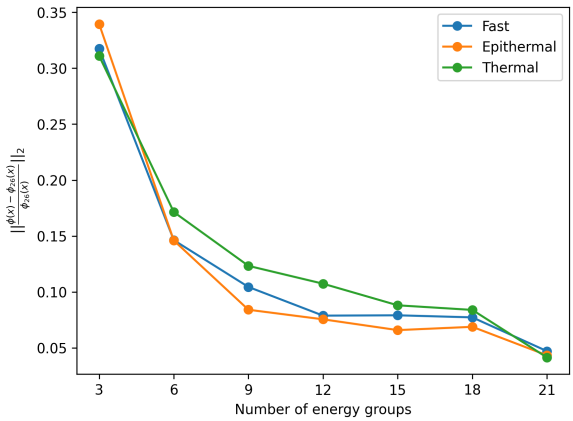

(a) 600K.

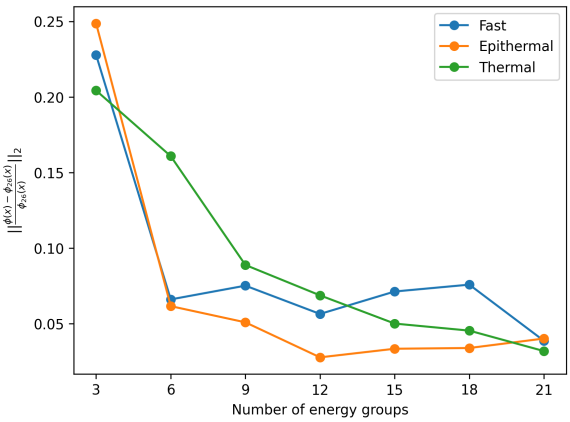

(b) 1200K.

Figure 7: No LBP case. L_2-norm relative error for different number of energy group structures.

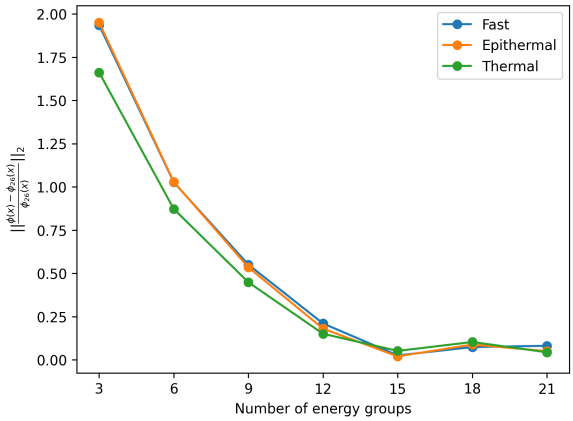

(a) 600K.

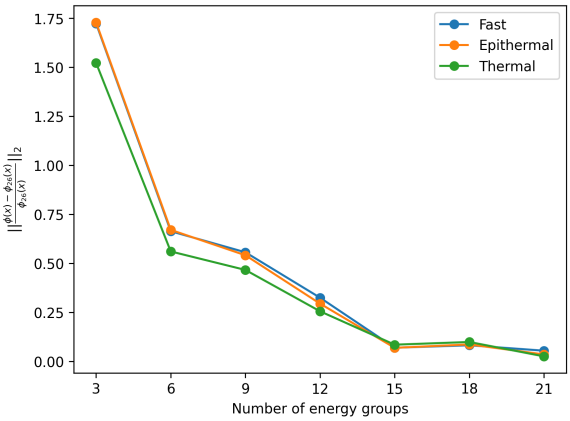

(b) 1200K.

Figure 8: LBP case. L_2-norm relative error for different number of energy group structures.

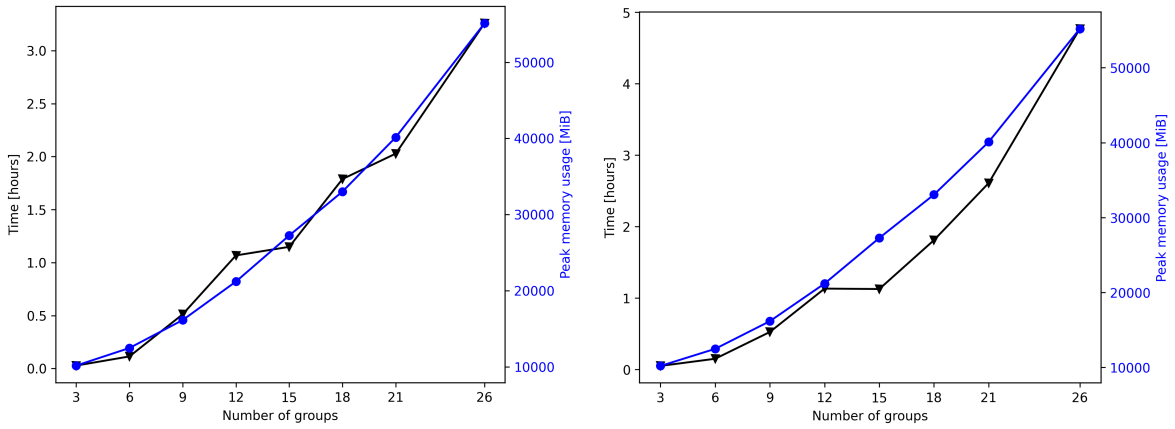

(a) No LBP and 600 K.

(b) LBP and 600 K.

Figure 9: Computational time and memory requirements for different number of energy group structures.

Table 3: Parametric study on the energy group limits. Values expressed in percentage.

LBP	Temperature [K]	Flux	15a	15b	15c	15d	15e
No	600	Fast	7.9	8.0	8.2	8.1	9.1
		Epithermal	6.6	6.5	8.6	8.2	9.2
		Thermal	8.8	8.5	10.6	10.7	12.9
	1200	Fast	7.1	7.7	5.7	5.1	4.5
		Epithermal	3.3	3.9	6.2	5.1	3.4
		Thermal	5.0	4.7	8.5	8.2	8.4
Yes	600	Fast	24.0	24.8	2.6	2.3	3.7
		Epithermal	21.0	21.7	2.0	1.6	2.7
		Thermal	18.1	18.8	5.2	5.5	5.7
	1200	Fast	36.2	37.3	6.9	6.6	25.9
		Epithermal	33.2	34.2	6.9	6.5	25.1
		Thermal	29.6	30.6	8.5	8.3	20.3
Weighted average			17.3	17.8	6.3	6.0	10.8

References

[1] Christophe Geuzaine and Jean-François Remacle. Gmsh: a three-dimensional finite element mesh generator with built-in pre- and post-processing facilities., June 2020.

[2] Nam-il Tak, Min-Hwan Kim, and Won Jae Lee. Numerical investigation of a heat transfer within the prismatic fuel assembly of a very high temperature reactor. *Annals of Nuclear Energy*, 35(10):1892–1899, October 2008.